MHD Phenomena and Disruption Characteristics in SST-1 Early Plasma

J.R Dhongde[1], M. Bhandarkar[1], S. Pradhan[1], S. Kumar[1]

[1]Institute for Plasma Research, Gujarat, India

E-mail contact of main author: jasraj@ipr.res.in

Abstract. Steady State Superconducting Tokamak (SST-1) is a medium size Tokamak (R_0/a=1.1/0.2, B_T~1.5T to 3T, I_P ~ 102kA) in operation at the Institute for Plasma Research, India. SST-1 has been consistently producing plasma currents in excess of 100kA, with Plasma durations above 250ms and a central magnetic field of ~1.5T in recent experimental campaigns of 2016. Investigation of experimental data measured using discrete in-vessel Poloidal and Toroidal Mirnov coils suggests the presence of MHD instabilities in SST-1 plasma. The Mirnov coil data have been analyzed using Fast Fourier Transform analysis, time resolved frequency analysis using wavelet spectrogram, Singular Value Decomposition (SVD) and Mirnov Phase Comparison method with an objective of investigating Magneto hydrodynamic phenomena in large aspect ratio (R/a > 5.5) plasma column such as formed in SST-1 plasmas. The analysis clearly explains the behavior of MHD instabilities observed (i.e. tearing mode with m/n=2/1), oscillation frequencies (in the range of ~ 5-7 kHz), growth rate and the island width in SST-1 Plasma etc. Onsets of (minor, major) disruptions triggered by MHD instabilities have been correlated with other diagnostics such as Soft-X ray, ECE, Hα and Density etc. The observations have been cross compared with the theoretical calculations based on Rutherford nonlinear theory and are found to be in good agreement. These results specific to high aspect ratio tokamak plasmas would be useful to future devices.

1. Introduction

Steady State Superconducting Tokamak (SST-1) is a medium size tokamak in operation at Institute for Plasma Research, India [1]. During evolution of plasma currents (Ip) in SST-1 experiments, SST-1 came across different phenomena of magneto hydrodynamic (MHD) instabilities [2]. These instabilities lead to disruptions and are in general limiting factors for improving plasma parameters such as Ip, beta (β), pressure gradient (ΔP) etc. Disruptions pose major concerns in operations of tokamak since large forces act on vacuum vessel with large amount of plasma energy getting deposited on plasma facing components i.e. operational lifetime of components. Many of the tokamaks and the fusion community have studied and explored the disruptions, MHD instabilities, avoidance of disruptions, mitigation strategies etc. These topics are relevant to present day tokamaks and for future large tokamak reactors such as International Thermonuclear Experimental Reactor (ITER) [3]. For steady state operation of SST-1, understanding of MHD instabilities and characteristics is important. Earlier different researchers and tokamaks have reported disruptions and MHD instabilities getting developed while approaching operational limits (e.g. density limit, β limit, q limit), fast density or current rise, error fields, influx of impurities from first wall etc. [4,5].

This paper presents the MHD phenomena observed and corresponding disruption characteristics in SST-1 experiments at the values of edge safety factor $2.4 \leq q_a \leq 4$. Earlier works [2] in SST-1 mention MHD characteristics (mode frequency, mode number, island width, growth rate etc.), different MHD regimes, mode evolutions and correlation of observation with other tokamaks. This paper along with MHD characteristics also proposes a probable physical processes or initiating events leading to disruptions. Section 2 includes a brief description of experimental set up, operational regime and diagnostics. Section 3

consists of multiple sub-sections putting light on MHD phenomena (e.g. saw teeth, saw teeth with Mirnov oscillations) with onsets of disruptions correlated with different diagnostics, MHD characteristics, time scales along with theoretical results. Section 4 proposes and discusses a probable physical process (an initiating event) leading to disruption and followed by general conclusions in section5.

2. SST-1 experiments and diagnostics

SST-1 is operated in limiter configuration (Graphite limiters) with plasma facing components as a first wall. It has 16 toroidal field (TF) superconducting coils responsible for providing required toroidal magnetic field (B_T ~ 1.5T to 3.0T) and a pair of vertical field coils for providing equilibrium field to plasma column. The breakdown of Hydrogen (H_2) gas plasma is initiated with Electron Cyclotron Heating (ECH) pre-ionization employing 42GHz Gyrotron in fundamental mode (Heating power ~75kW-200kW), with the start up being assisted with a resistive Ohmic transformer in low loop voltage (0.3 V/m) scenario. In some of the experiments, Lower Hybrid Current Drive (LHCD) power ~ 100kW-150kW is launched in the flat top region of established plasma current for current drive.

SST-1 is equipped with Electron Cyclotron Emission (ECE) diagnostics (Radiometer E-Band, 74-86GHz), Spectroscopy system (for temporal evolution of H_α, H_β, O_I, O_{II}, C_{II} etc. line emissions), Soft X-ray , Hard X-ray diagnostics (Nal(TI) Scintillator detector, 70keV-10MeV) and Density diagnostics (Heterodyne and Homodyne) , Infrared imaging of inboard-outboard limiters, Bolometer diagnostics etc. Also, it has discrete in vessel Mirnov coil arrays to measure poloidal magnetic fluctuations. Two arrays are poloidally distributed; one comprises 24 separate Mirnov coils (M24) and the second comprises separate 8 Mirnov coils (M8). Single array of 4 separate Mirnov coils (N4) is placed toroidally inside vessel. Each Mirnov coil consists of 34 turns of 0.6mm diameter copper wire wound (two layers for M8, N4 arrays and single layer for M24 array) on a rectangular former with an effective area of ~ $300mm^2$. All the Mirnov coil data are acquired at 100 kHz sampling rate with 14bit resolution for M8, N4 arrays and 16bit resolution for M24 array. Mirnov coil oscillations from M24 array are largely analyzed in this study for MHD characteristics.

3. Observed MHD phenomena and disruption characteristics

SST-1 plasma experiment with representative shot#7607 is shown in Fig.1. The main parameters for this shot are B_T ~ 1.5T, Ip ~ 102 kA, ECRH power ~190 kW, vessel pressure (H_2) ~ $8x10^{-6}$ mBar and loop voltage ~ 2.4 V. Investigation of experimental data using Mirnov coil array, soft x-ray diagnostics, loop voltage, ECE signals and hard x-ray signals lead to an observation of different MHD regimes (e.g. Saw Teeth, Saw teeth coupled with Mirnov oscillations).

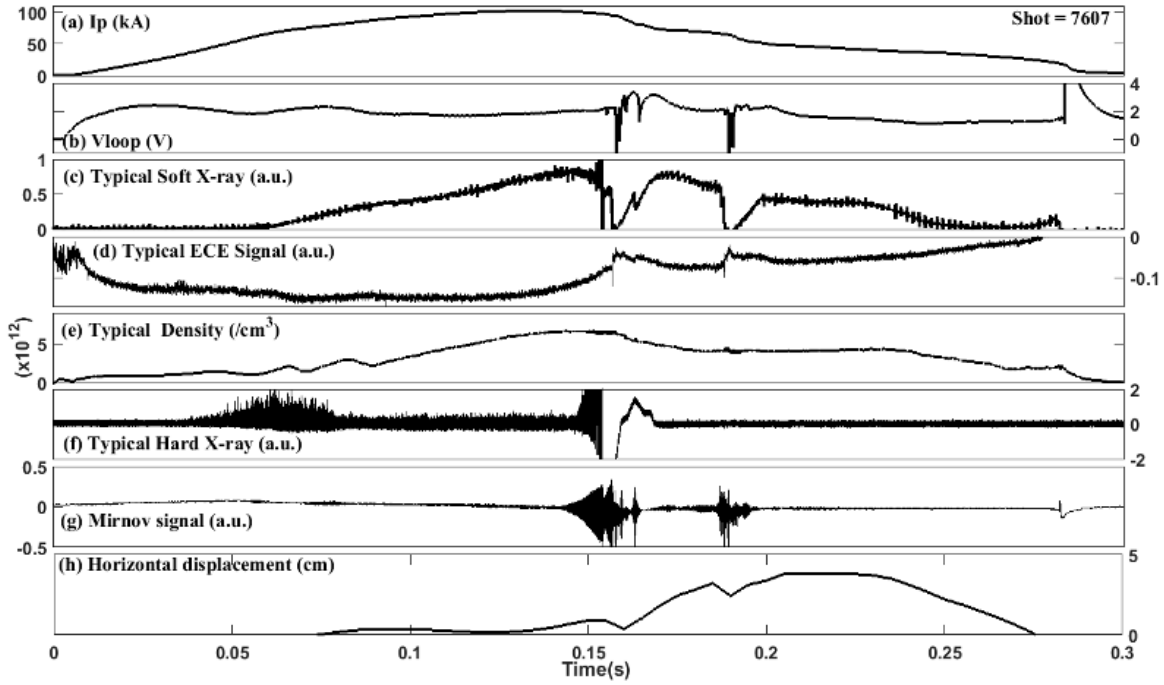

FIG.1. SST-1 shot no. 7607, (a) Plasma current, (b) Loop voltage, (c) Typical Soft X-ray signal, (d) Typical ECE signal, (e) Typical density, (f) Typical Hard X-ray signal, (g) Mirnov signal and, (h) Horizontal displacement

3.1. Saw teeth oscillations

During time interval 130-144ms of shot#7607 (Fig.2.b), saw teeth oscillations are seen in soft x-ray diagnostics suggesting an internal disruptions occurring in the core of the plasma. No significant oscillations were observed in Mirnov coils during this interval. We believe this to indicate presence of m/n=1/1 mode on q=1 surface. Similar observations are also reported by other tokamaks in low, moderate and high aspect ratio tokamaks [6,7,8,4].

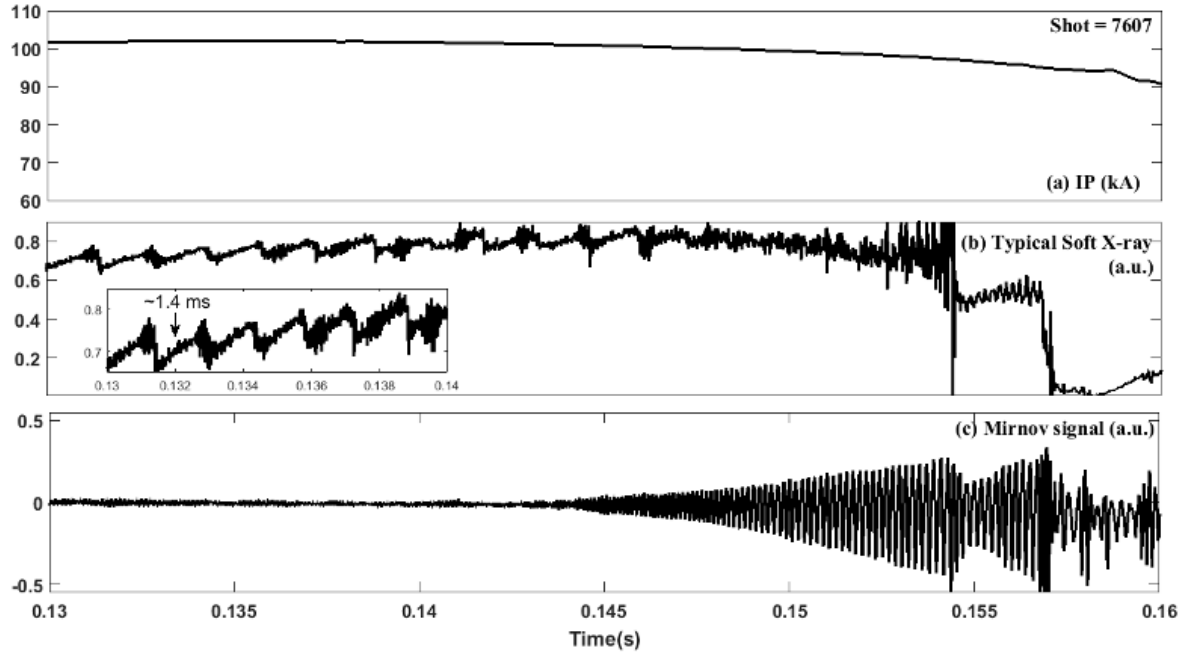

FIG.2. Shot no. 7607, (a) Plasma current, (b) Typical Soft X-ray signal and (c) Mirnov signal

q=1 resonant surface is R_s ~ 9.8 cm, computed considering current profile as J ~ $(1-(r/a)^2)^{\alpha}$ and q(r) profile as $q(r) = q(a) * \frac{(r/a)^2}{1-(1-(r/a)^2)^{\alpha+1}}$ (with α=3, a=0.2 m). The saw teeth relaxation effect is periodic with its period proportional to central density and can be estimated using empirical formula [9], $\tau_r(ms) = \left(\frac{1}{800}\right) n_e {R_s}^2 R_0$ (where n_e – electron density – 10^{14} cm^{-3}, R_s – rational surface in cm, R_0 in cm). Computed $\tau_r \sim 0.808\, ms$ is in reasonable agreement with experimentally observed saw teeth period ~ 1.4ms as shown in inset Fig.2.b despite considerable uncertainties. This regime seems to be macroscopically stable with good confinement properties.

3.2. Saw teeth coupled with Mirnov oscillations (m/n=2/1)

During time interval 144-155ms (Fig.2.c), presence of distinctive Mirnov oscillations growing in amplitude are observed. In this interval, soft X-ray signals remain similar to earlier region but having precursor oscillations increasing in amplitude. At about 154.3ms, sudden drop in soft X-ray signal and decrease in amplitude of Mirnov signal is observed. This thermal quench, followed by fall loop voltage suggests it as a minor disruption. Measured perturbation amplitude ($\tilde{B}_\theta$) to poloidal magnetic field (B_θ) at the detecting Mirnov coil is $\tilde{B}_\theta/B_\theta \approx 0.65\%$ just prior to minor disruption. Again during time interval 155-157ms (Fig.2.c), MHD activity detected by Mirnov coil is observed to increase with a significant rapid growth. Amplitude of $\tilde{B}_\theta/B_\theta \approx 1.0\%$ is observed just prior to major disruption.

Similar observations in number of tokamak experiments have reported that m/n=1/1 mode triggering different modes m/n=2/1, m/n=3/2, m/n=4/3 mode with or without saw tooth collapse and causing disruptions [10,11]. We observe similar phenomena in this region, m/n=1/1 structure triggering m=2, n=1 tearing mode and subsequently leading to minor and major disruptions.

3.3. MHD characteristics

MHD characteristics are analyzed using Mirnov coil data (with M24 array). The analysis includes Fast Fourier Transform (FFT) for understanding the dominant mode frequency, time resolved frequency analysis using wavelet spectrogram for temporal profile of dominant mode frequencies, Singular Value Decomposition (SVD) [12] and phase comparison method for spatial structure of dominant mode [13].

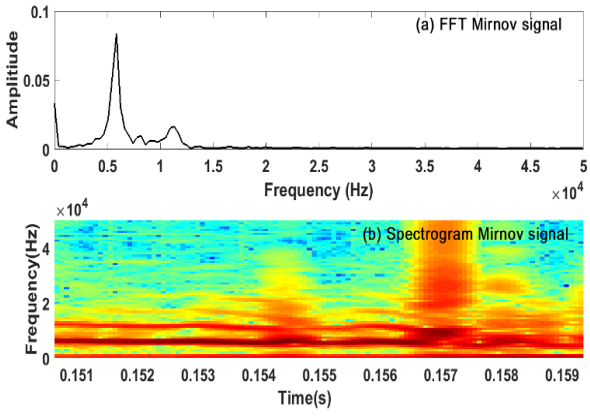

FIG.3. (a) Fourier Transform (b) Spectrogram – Mirnov signal

During interval 150-160ms, the dominant frequency of Mirnov oscillations associated with tearing mode is ~ 5.9 kHz with its harmonics as shown in Fig.3. Spatial analysis using SVD method during interval 155-156.5ms reveals m=2 island structure as dominant one as shown in polar plot of Fig.4.b. Fig.4.a. shows the corresponding time vector i.e. oscillations resulting from rotation of spatial structure of m=2 mode. Phase comparison of Mirnov coils also reveals m=2 mode as shown in Fig.5 and having rotation in the direction of electron diamagnetic drift.

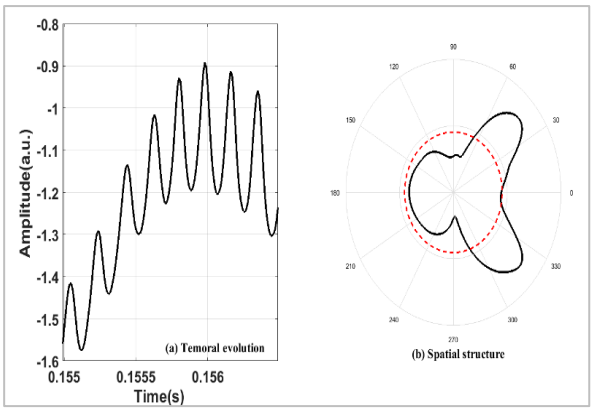

FIG.4. (a) Temporal evolution (b) Spatial structure showing m=2 mode

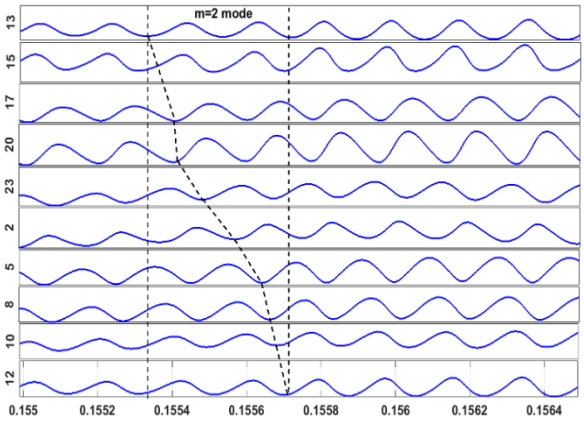

FIG.5. Phase comparison of Mirnov signals according to poloidal position (suggesting m=2 mode)

For Ohmically heated plasmas, the rotation frequency of magnetic perturbation is about the electron drift frequency [14], $f_{De} \propto \frac{(kT_{e0})}{eB_t a^2}$ (where, k is Boltzmann constant and T_{e0} is the central electron temperature). For SST-1, with B_T ~1.5 T, a=0.2 m and T_{e0} =360 eV, f_{De} ~ 6 kHz and is in reasonable agreement with observed on.

3.4. Time scales

One of the characteristics is the time scale on which the mode grows and leads to disruption. Typically, the growth times of the disruption precursors range from tens of microseconds to milliseconds order. Typical ideal time scale τ_A is given by Poloidal Alfven time, which is $\tau_A \equiv {}^{a}/_{V_A}$, (where V_A as Alfven velocity). Resistive diffusion time,$\tau_R \equiv \mu_0 a^2/\eta(0)$, with η(0) as the resistivity at the plasma center. For resistive tearing mode, the resistive timescale is given by [5,2]

$$\tau_S \cong \tau_R^{0.6} \times \tau_A^{0.4} \quad (1)$$

In SST-1, Alfven velocity is about 2.7×10^5m/s and η(0)= 1.89×10^{-7}Ωm from the classical Spitzer parallel resistivity, which value follows for T_e = 360 eV and Z_{eff} =2.5. With above mentioned values, we calculate τ_A = 0.7μs, τ_R = 0.2654s and τ_s = 1.586ms. The timescale for the non-linear growth of the m=2 mode τ_g is ~ 670μs, which can be considered as an approximation of the timescale τ_g for linear growth. Approximated experimental value of τ_g is less than half of linear theoretical one τ_s = 1.586ms and satisfies the general relation between linear MHD mode growth timeτ_g, ideal timescale τ_A and resistive diffusion time τ_R as given below

$$\tau_A < \tau_g < \tau_R \quad (2)$$

3.5. Island width (W), dW/dt and Island structure

The classical tearing mode is a current driven instability which involves magnetic reconnection. Magnetic reconnection changes magnetic field topology with nested flux surfaces along the resonant surface forming magnetic islands [13].

The magnetic island width can be estimated by [6,7]

$$W = r_c \sqrt{\frac{\tilde{B}_\theta}{B_\theta}} \quad (3)$$

Where, r_c is the radius of the detecting Mirnov and $\tilde{B}_\theta/B_\theta$ is ratio of measured perturbation amplitude to poloidal magnetic field magnitude at the detecting Mirnov coil. The resonant surface for q=2 surface for earlier mentioned q(r) profile is $R_s \sim 16.8$ cm. Fig.6. Shows time evolution of W during the time interval 150-160ms. The linear tearing mode growth rate (γ) can be obtained by fitting an exponential function to the time evolution of W [15]. Estimated growth rate $\gamma \sim 450\ s^{-1}$ (Fig.6.) is observed during interval 156-157ms. The linear tearing width is given as [16]

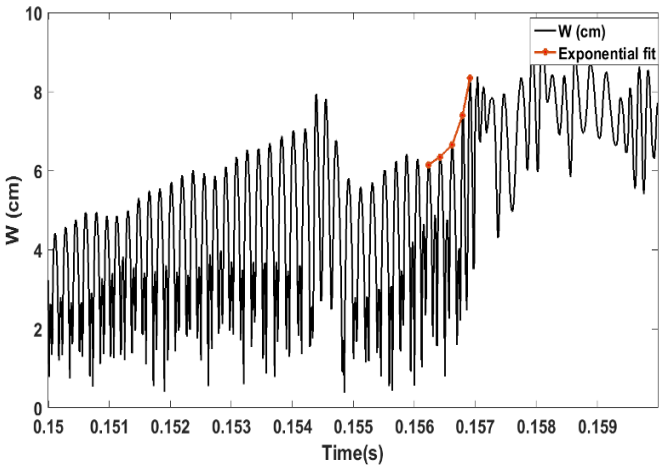

FIG.6. Time evolution of island width of m=2 mode (black) with exponential fit (red) during interval 156-157ms.

$$\delta_t \sim \left(\frac{\gamma \tau_A^2}{\tau_R}\right)^{1/4} \quad (4)$$

In above case, we estimate $\delta_t \sim 1.7$mm. Researchers also report the layer width of being of the order of ion-larmor radius (i.e. of the order of millimeter) [8].

The growth rate dW/dt estimated by Rutherford non-linear theory is given by [17]

$$\frac{dw}{dt} \approx \frac{1}{\mu_0} \eta \Delta' \quad (5)$$

Where, η is the resistivity and Δ' is the jump in logarithmic derivative of perturbed helical flux function ψ across the resonant surface. In the absence of an accurate knowledge of the current profile at the relevant time we assume Δ' is of order $1cm^{-1}$ [17,2]. If we make further assumption that Δ' does not change significantly during the rapid growth phase then $dW/dt \approx 0.15 \times 10^4\ cm \cdot s^{-1}$.

Fig.7. shows island structures as computed flux contours for m=2 tearing mode at three different time instants (in the interval 156-157ms) with corresponding perturbation amplitude prior to disruption. These flux contours are superposition of helical flux function (Ψ_h) and perturbed poloidal flux function in general form ($\Psi r\, cos\xi$) [18,19]. At present, island widths computed from flux contours are not in agreement the ones computed from Eq.(3). The possible reason could be absence of current density and q(r) profile information.

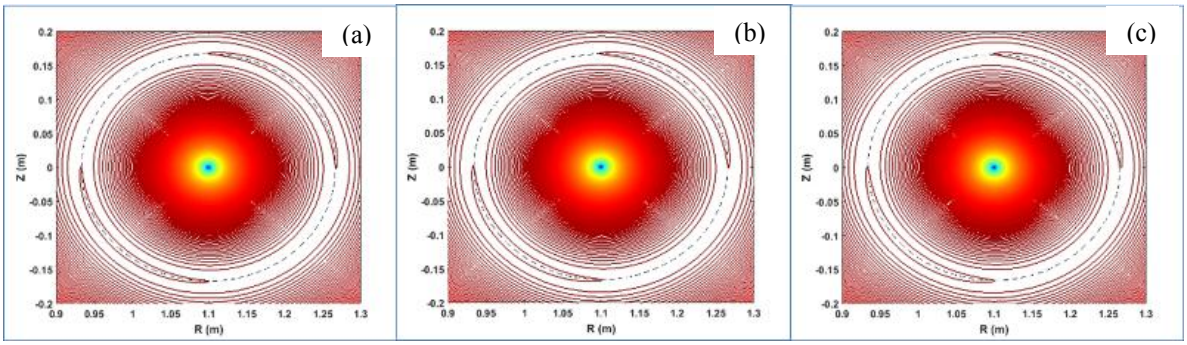

FIG.7. Computed flux contours for m=2 tearing mode with (a) $\tilde{B}_\theta/B_\theta \approx 0.57\%$ at ~156.2ms (b) $\tilde{B}_\theta/B_\theta \approx 0.83\%$ at ~156.8ms (c) $\tilde{B}_\theta/B_\theta \approx 1.05\%$ at ~157ms

4. Discussion

Disruption scenario for shot#7607 is shown in Fig.8. Researchers have reported evolution of a tokamak discharge with different phases and schemes of possible precursor scenarios or possible initiating events leading to disruptions [5]. Similarly, one can see an initiating event or pre cursor phase followed by a thermal quench and then current quench in shot#7607 as shown in Fig.8.

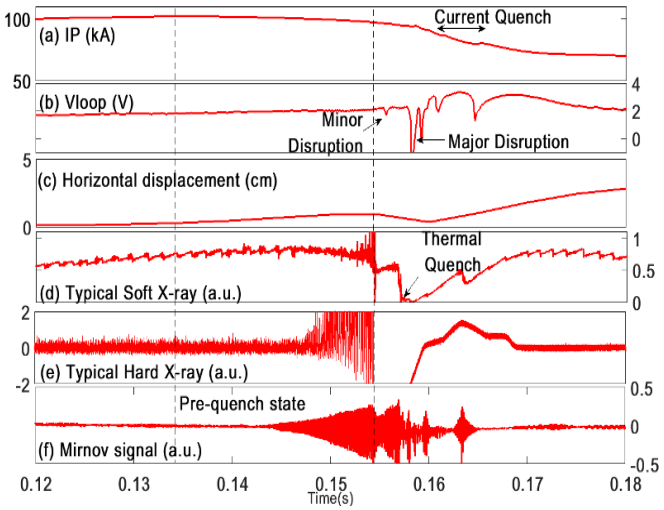

FIG.8. Disruption scenario for shot no. 7607 with Pre cursor, thermal quench and current quench

Before initiating event or pre-quench state (before ~140ms), plasma seems to be macroscopically stable, with nearly flat top current ~ 97 kA. During interval 140-154ms of pre quench state, m=2 mode grows along with m=1. Hard X rays are observed to increase along with change in plasma radial position. At ~ 154.3ms, soft crash is observed, leading to minor disruption as observed in drop of loop voltage. Recovery of temperature profile after minor disruption is observed during interval ~ 154.4-157ms, but simultaneously m=2 mode is observed to grow on much faster time scale. This m=2 mode grows and saturates at island width ~ 8 cm. Possible stronger interaction between islands and limiter leads to bigger thermal quench at ~ 157.1ms. After heat release during thermal quench, current quench (Ip ~ 95kA to ~ 80kA) occurs with poloidal magnetic field energy released. A negative voltage spike in loop voltage suggests it to be a major disruption. Probable physical processes happening during disruption [9] is shown in Fig.9.

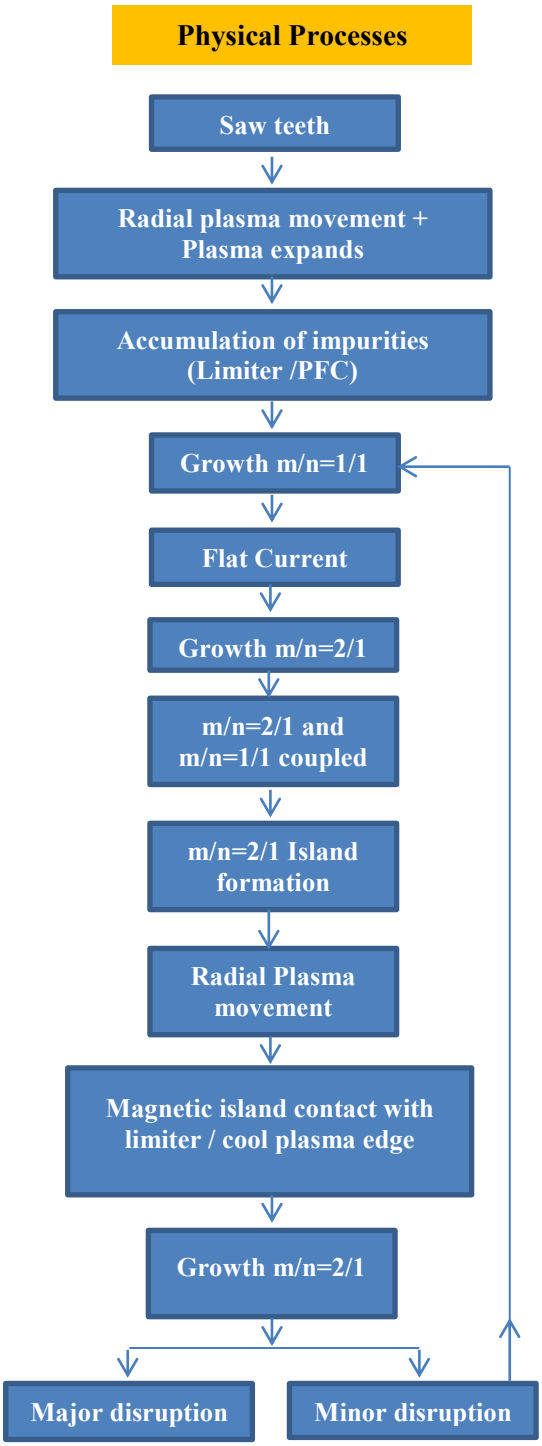

FIG.9. Probable physical processes leading to disruption

5. Conclusion

This work described and discussed different MHD regimes (saw teeth, saw teeth coupled with Mirnov oscillations) at the value of edge safety factor $2.8 < q_a < 4$. The observed saw teeth period ~ 1.4ms is in reasonable agreement with estimated using empirical formula $\tau_r \sim 0.808\, ms$. Experiment observes m=1 mode and m=2 mode with stronger amplitude. m=2, n=1 mode activity in the outer region is significantly strong to cause minor and major disruptions. The approximated experimental value of τ_g ~ 0.67ms is nearly half of τ_s = 1.586ms and satisfies the condition $\tau_A < \tau_g < \tau_R$, where τ_A = 0.7μs, τ_R = 0.2654s. Disruption scenario observed suggests radial plasma displacement due to inadequate radial position control as an initiating or precursor event for disruption. All the above aspect will be useful in disruption avoidance and disruption mitigations in SST-1.

Acknowledgement

Authors wish to thank electronics group, data acquisition group, diagnostics group and SST-1 team for all the help and useful discussions.

References

[1] S. Pradhan, Z. Khan, V.L. Tanna, et al. Nuclear fusion 55, No.10 (2015) 104009.

[2] J Dhongde, M Bhandarkar, et al., Fusion Engineering Design 108 (2016) 77-80.

[3] T.C. Hender, J.C Wesley, J. Bialek, et al Nuclear fusion 47 (2007) S128-S202.

[4] B.B. Kadomstev, Plasma Physics Series, Tokamak Plasma: A complex physical system, 1992, pp. 109-123.

[5] F.C. Schuller, Plasma Physics and Controlled Fusion 37 (1995) A135-A162.

[6] EQUIPE TFR, Nuclear fusion 17, No.6 (1977) 1283-1296.

[7] A. D. Cheetham, et al. Australian Journal of Physics 39, No.39 (1986) 35-55.

[8] Tokamaks, John Wesson, Clarendon Press-Oxford, 1987, pp.365-374.

[9] B.B. Kadomtsev, Plasma Physics and Controlled Fusion 26, No.1A (1984) pp. 217-226.

[10] M. Asif, X. Gao et al., Physics Letters A 342 (2005) 175-180.

[11] F. Karger, et al. Review of Disruptive Phenomena in Pulsator, Proceedings of IAEA symposium on Current Disruption in Toroidal devices, Garching, February 1979, A4.

[12] C Nordone, Plasma Physics and Controlled Fusion 34 (1992) 1447-1465.

[13] Active Control of Magneto-hydrodynamic Instabilities in Hot Plasmas, Valentin Igochine, Springer Series, 2015,pp. 9-103.

[14] Qingwei Yang, L. Yan et.al, Brazilian Journal of Physics 32, No.1(2002) 160-164.

[15] Pravesh Dhyani, J. Ghosh et al. Nuclear Fusion 54 (2014) 083023(5pp).

[16] Y.Z.Zhang, R.Denton, S.M.Mahajan, Physical review letters 65, No.23 (1990) 2877-2880

[17] A.D. Cheetham, S.M. Hamberger, Nuclear Fusion 27 No.5 (1987) 843-847.

[18] Richard Fitzpatrick, Physics Plasmas 2, No.3 (1995) 825-838.

[19] Magneto hydrodynamic stability of tokamaks, H. Zohm, Wiley, 2015, 123-140.